

Application of Model Based Predictive Control for a Rotary Tablet Press

Ioana Nașcu

Department of Automation
Technical University of Cluj Napoca,
Academy of Romanian Scientists,
Romania
ioana.nascu@aut.utcluj.ro

Ioan Nașcu

Department of Automation
Technical University of Cluj Napoca
Cluj Napoca, Romania
ioan.nascu@aut.utcluj.ro

Zoltan K. Nagy

Davidson School of Chemical Engineering
Purdue University
West Lafayette, USA
znagy@purdue.edu

Abstract— Recently, the pharmaceutical manufacturing is going through a transition from classic batch manufacturing to continuous manufacturing, that is a faster as well as a more effective approach. The presented work establishes the foundation for cutting-edge advanced Quality-by-Control model-based predictive control strategies applied on a continuous manufacturing rotary tablet press process. Advanced model predictive control strategies are capable in facilitating the switch to Industry 4.0 by assuring a Quality-by-Control approach. To control the continuous manufacturing of solid dosage forms within the pharma industry different advanced model based predictive control strategies including unconstrained as well as constrained MPC are developed and implemented. The model that is used to design the control strategies is calibrated and validated by using actual data taken from a pilot plant. The results present good performances of the developed controllers: increased efficiency of the process as well as flexibility, a decrease in the environmental impact even when accounting for uncertainties in the process, measurement sensor noise as well as disturbances

Keywords— process control, model based predictive control, pharmaceuticals, rotary tablet press, Quality by Control

I. INTRODUCTION

The pharmaceutical industry is composed of very complex processes that are required to work close to regulatory and operational constraints which have to meet high standards of quality for its products. Moreover, it has a very unique economic and regulatory environment and it has to deal with highly intricate as well as integrated processes, product variations, uncertainty in the process/model, production targets that vary, and raw material variability [1–3]. Pharmaceutical manufacturing has traditionally used a batch processing type of approach, in which the quality control is done in a quality-by-testing type of manner where quality of the drug product is evaluated in the last step of the process of each individual batch.

Continuous manufacturing is beginning to substitute batch manufacturing within the pharma industry. This shift is driven by the necessity for enhanced sustainability, cost-effectiveness, developing economically viable routes for personalized medicine such as tailored treatments for smaller patient groups along with innovations in the latest manufacturing technology [4–6]. As a result of this transition there will be a progression towards quality-by-control (QbC) which is composed in the design and operation of robust manufacturing systems which use active process control systems based on robust process design. This change represents a significant step toward smart manufacturing [7–11].

The presented work represents the basis for cutting edge Quality-by-Control model predictive control (MPC) techniques for a continuous tablet manufacturing process. To begin with, a model of the process has to be determined, then using real plant data the model has to be calibrated and validated. This model is then used for the design of advanced MPCs with an emphasis on robustness, specifically in managing uncertainties, efficient rejection of disturbances, time delays that are variable, as well as explicit incorporation of constraints. As a result, the pharmaceutical manufacturing industries will benefit greatly from this, especially in light of the strict rules set out by the FDA (Food and Drug Administration).

This paper has the following structure: the development of the mathematical model for the process, the model based predictive control method as well as the predictive algorithm design are presented in the second Section. The next Section depicts the performance analysis for the developed control strategies for step setpoint changes, measurement noise influence and disturbances rejection. Finally, Section IV concludes the main result of this paper.

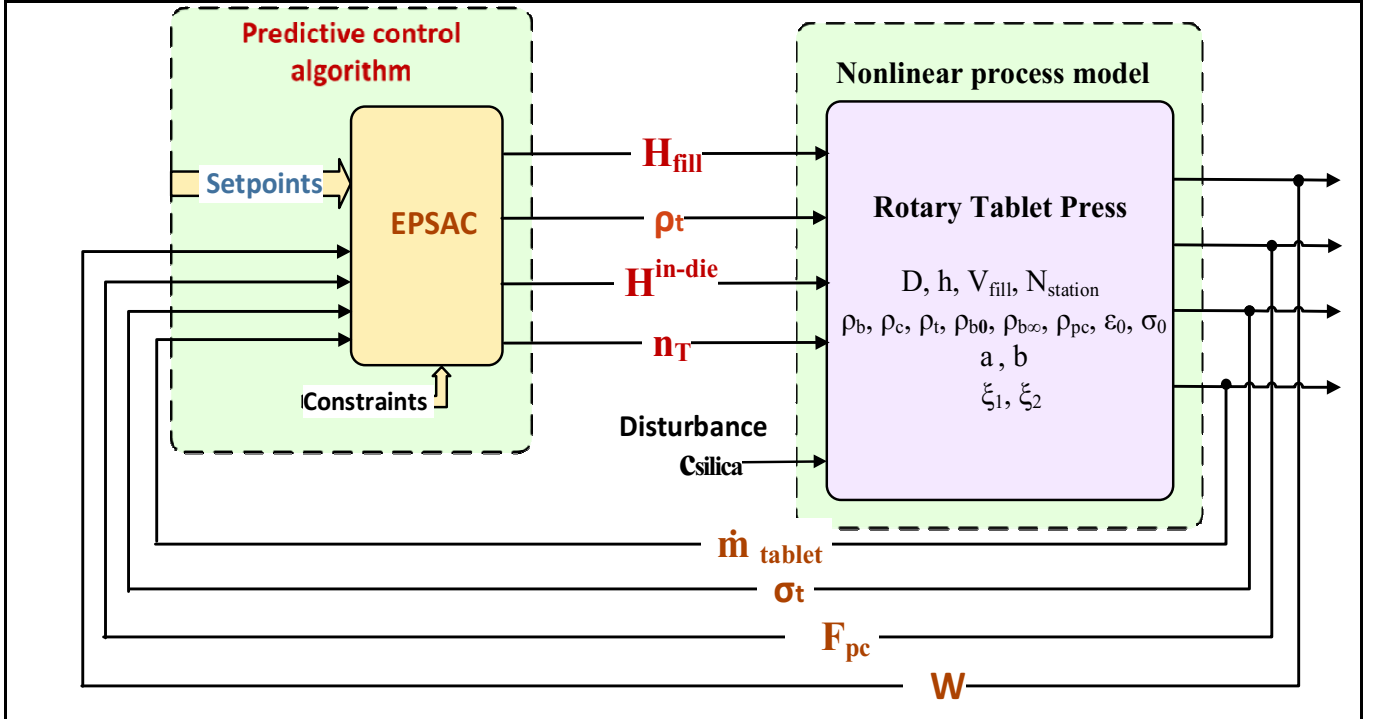


Fig. 1. The control diagram of the rotary tablet press

II. THEORETICAL BACKGROUND

A. Process Model

The lubricant/glidant feeder, as well as the the rotating tablet press, constitutes a crucial element in the pharmaceutical manufacturing industry. Its primary role is to decrease frictional forces and enhance powder flow throughout die filling, which facilitates the mechanical compression necessary for forming solid tablets. Mechanistic models are employed to monitor as well as control key tablet characteristics, like tensile strength and tablet porosity, by assessing the impact of glidants during both the die filling and compression phases [12].

Equation (1) is applied to calculate the convex tablet weight (W), considering the shallow cup depth of the Natoli D-type tooling

$$W = \rho_b V_{fill} \left(1 - \xi_1 \frac{n_T}{n_F} + \xi_2 \frac{H_{fill}}{D} \right) \quad (1)$$

In equation (1) V_{fill} , ρ_b , H_{fill} , n_T , n_F , and D are the die cavity volume, powder bulk density, dose position, turret speed, feed frame speed, and the die diameter. The parameters ξ_1 and ξ_2 represent model parameters which are determined from experimental data. The bulk density is influenced by the glidant concentration and the mixing conditions. For Natoli D-type tooling, the die cavity volume is determined using the following expression:

$$V_{fill} = \frac{\pi D^2 H_{fill}}{4} + \frac{\pi h \left(\frac{3D^2}{4} + h^2 \right)}{6} \quad (2)$$

, h denotes the cup depth. To calculate the production rate of the tablet, (\dot{m}_{tablet}) the following equation is used:

$$\dot{m}_{tablet} = W n_T N_{station}, \quad (3)$$

where $N_{station}$ denotes the number of the turret stations that are accessible. To compute the pre-compression force (PCF) we will use:

$$F_{pc} = \frac{\pi D^2}{4b} \left[\frac{\rho^{pc} - \rho_c}{\rho^{pc} (a-1) + \rho_c} \right] \quad (4)$$

The constants a and b denote the Kawakita constants [13]. The critical density is ρ_c and ρ^{pc} , corresponds to the relative density during pre-compression, determined using:

$$\rho^{pc} = \frac{W}{V^{pc} \rho_t} \quad (5)$$

and

$$V^{pc} = \frac{\pi D^2 H^{pc}}{4} + \frac{\pi h \left(\frac{3D^2}{4} + h^2 \right)}{3} \quad (6)$$

H^{pc} is the true powder density, while ρ_t defines the thickness of the pre-compression. As a result, the main compression force (F_{punch}), is calculated with:

$$F_{punch} = \frac{\pi D^2}{4b} + \left[\frac{\rho^{in-die} - \rho_c}{\rho^{in-die} (a-1) + \rho_c} \right] \quad (7)$$

The in-die relative density ρ^{in-die} is obtained by the subsequent relation:

$$\rho^{in-die} = \frac{W}{V^{in-die} \cdot \rho_t} \quad (8)$$

and

$$V^{in-die} = \frac{\pi D^2 H^{in-die}}{4} + \frac{\pi h \left(\frac{3D^2}{4} + h^2 \right)}{3}. \quad (9)$$

The thickness during main compression, H^{in-die} is utilized to calculate the tablet density ρ^{tablet} , through the elastic recovery, ε_ρ :

$$\rho^{tablet} = (1 - \varepsilon_\rho) \rho^{in-die}. \quad (10)$$

Mixing conditions of the glidant have minimal effect on the elastic recovery, which is determined using:

$$\varepsilon_\rho = \varepsilon_0 \frac{\rho^{in-die} - \rho_{c,\varepsilon}}{1 - \rho_{c,\varepsilon}} \quad (11)$$

The relative density without elastic recovery is denoted by $\rho_{c,\varepsilon}$ while the in-die elastic recovery when at full contraction is ε_0 . Tensile strength σ_t which is influenced by lubricant conditions, is calculated using the expression:

$$\sigma_t = \sigma_0 \left(1 - \left(\frac{1 - \rho^{tablet}}{1 - \rho_{c,\sigma_t}} \right) e^{(\rho^{tablet} - \rho_{c,\sigma_t})} \right). \quad (12)$$

The parameter σ_0 represents tensile strength at zero porosity, while σ_{c,σ_t} represents the relative critical densities if no tensile strength is exhibited by the tablets.

The concentration of the glidant c_l dependent on bulk density, is determined through the following equation:

$$p_b = p_{b,\infty} - \frac{p_{b,\infty} - p_{b,0}}{1 + C_p} \quad (13)$$

$\rho_{b,0}$ and $\rho_{b,\infty}$ denote bulk densities at zero and infinite shear strain, respectively. The lumped parameter C_p reflecting glidant conditions, can be calculated using:

$$C_p = \frac{c_l^{r_1} (\gamma + \gamma_0)^{r_2}}{r_3} \quad (14)$$

γ represents the shear applied on the powder during mixing and γ_0 represents initial shear strain prior to mixing. Moreover, parameters r_1 , r_2 , and r_3 are fitting parameters.

For this study, a Natoli NP-400 tablet press as well as a SOTAX AT4 tablet tester are utilized for the production of tablets as well as for data experiment data collection that are performed under steady-state conditions. To estimate actual model parameters, which were subsequently used to calibrate and refine the model for simulation purposes, data collected from the performed experiments is used.

B. Extended Prediction Self Adaptive Control

Figure 1 illustrates the hierarchical control system layers developed for the study. The Model Predictive Control (MPC)

was implemented using the Extended Prediction Self Adaptive Controller (EPSAC) method, as detailed in [14]. The predictive control algorithm has four inputs and also four outputs. The control algorithm was derived through the minimization of the cost function:

$$J(U) = \sum_{i=1}^4 \sum_{k=N_{1i}}^{N_{2i}} [r_i(t+k) - y_i(t+k)]^2 + \sum_{j=1}^4 \sum_{k=0}^{N_{uj}-1} \lambda_j \cdot [4u_j(t+k|t)]^2 \quad (15)$$

where U represents a vector containing the controller outputs, r_i represents the setpoints sequences, u_i represent the controller outputs/process inputs and y_i represent the outputs of the process.

If $J(U)$ is minimized with respect to the U vector, the optimal problem solution is given, and the current control actions can be determined for unconstrained conditions.

When process constraints are present, the control action calculation becomes a constrained optimization problem, represented as (15) subjected to a linear form inequality $A \cdot U < b$, where A represents a predefined matrix and b a predefined vector, both dependent on the considered constraints. This optimization task, known as quadratic programming, is commonly addressed using quadratic programming methods. Constrained optimization typically delivers superior results compared to basic clipping procedures [14].

C. Control Design

To design the predictive control algorithm, the following parameters were used: the control horizons of the four outputs $N_{ui}=1$ and the process output prediction horizons $N_{21}=5$, $N_{22}=N_{23}=N_{24}=10$. To select the output control horizons as well as the prediction horizons one must consider the process characteristics and the requested closed-loop performances. For the case where we have processes that do not have unstable or underdamped poles, such as the current case, $N_u=1$ is usually adequate when N_u is set up. Measured data is obtained from the plant at every 1 second therefore the sampling time was set up to $T_s = 1$ second. All manipulated inputs will be subject to constraints. One of the most important advantages in using model predictive controllers is that is the seamlessly integration of these constraints. The specific constraints applied to the manipulated inputs for the process include: dosing position, which can be in the range [6mm - 14mm], pre-compression thickness which can be in the range [0.5mm - 14mm], main compression thickness which can be in the range [0.5mm - 6mm], and turret speed which can be in the range [0 rpm - 60 rpm].

III. RESULTS

This study implements the process mathematical model described in Section II.A, which involves four inputs of the process and four outputs. A toolbox of the MATLAB (System Identification) is utilized to develop a linear process model with multiple inputs and multiple outputs (MIMO). This linear representation is subsequently employed for the predictive controller design. The predictive algorithm controls four key variables of the process: the weight of the tablet (Twei), the

pre-compression force (Pcom), the rate of production (Prod), and tensile strength (Tstr). The controller outputs/process inputs include dosing position (Dose), pre-compression thickness (Ptck), main compression thickness (Mtck), and turret speed (Tret). For the strength of the tensile, sensor measurements are recorded every second. The process parameters used in this model, determined using extensive experimental measurements, include: $\rho_b = 0.365 \text{ [g/cm}^3]$, $\rho_c = 0.26$, $a = 0.81$, $1/b = 10.26 \text{ [Mpa]}$, $\epsilon_0 = 0.08$, $\rho_t = 1.532 \text{ [g/cm}^3]$, $\rho_{c,e} = 0.57$, $\rho_0 = 0.57$, $\rho_\infty = 0.61$, $\sigma_0 = 11.67 \text{ [Mpa]}$, $b_1 = 0.31$, $b_1 = 0.38$, $b_2 = 8.4$, $\rho_{b,\infty} = 0.45 \text{ [g/cm}^3]$, $\rho_{b,0} = 0.33 \text{ [g/cm}^3]$, $r_1 = 0.36$, $r_2 = 1.384$, $r_3 = 23.319$, $\xi_1 = 0.036$, $\xi_2 = 0.03$.

A. Setpoint tracking

The performances of the control strategy designed in this work is evaluated through setpoint changes. At time $t = 50$ seconds, the tablet weight setpoint shifts from 0.225 g to 0.255 g; at the moment $t = 100$ seconds, the pre-compression force changes from 370 N to 670 kN; at $t = 200$ seconds, the production rate increases to 8.4 kg/h from a value of 7.4 kg/h; and at $t=300$ seconds, the tensile strength setpoint rises from 5.6 MPa to a value of 6.4 MPa.

One of the biggest advantages in using model predictive controllers is their capability of incorporating constraints explicitly. For a more in depth understanding of the differences of the unconstrained and constrained MPC two cases are considered for setpoint changes in this work: (i) unconstrained MPC, presented in Figure 2 and 3 and (i) constrained MPC, presented in Figure 4 and 5.

Fig. 2 and 3 depict the response of the closed loop system to changes in the setpoint using the unconstraint EPSAC controller when no noise is present in the measured outputs. Fig. 2 highlights the step response for the controlled variables, revealing the interdependence of the outputs. A change in one output influences the others, which is observable in both constrained and unconstrained MPCs. Fig. 3 demonstrates the control action, where the strongest effect on all outputs is triggered by a tablet weight setpoint change at 50 seconds. For the unconstrained case it can be observed from Fig 3 that the outputs have no limits on them therefore the control strategies present a fast response time.

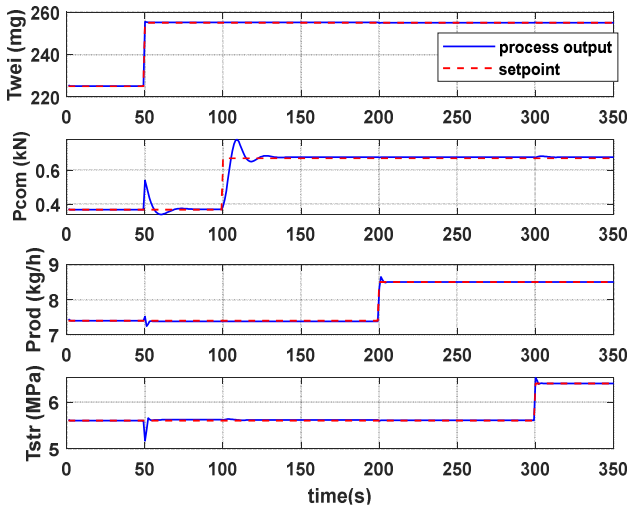


Fig. 2. No constraints reference tracking - process outputs

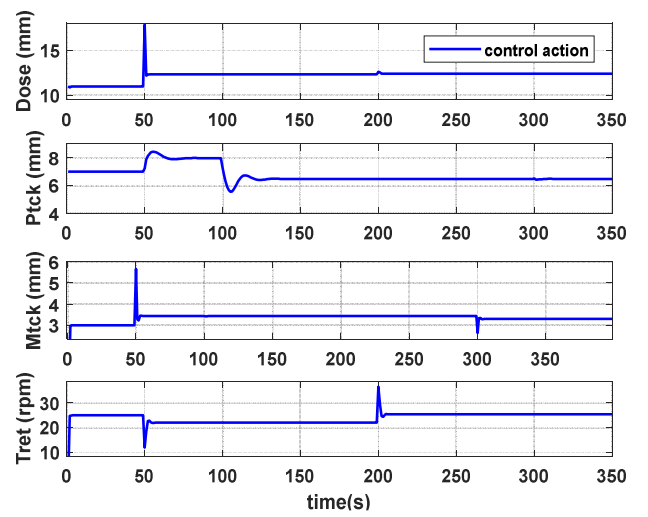


Fig. 3. No constraints reference tracking - controller outputs.

The response of the closed-loop system when dealing with setpoint changes under the constrained EPSAC control, without noise in the measured outputs, is presented in Fig. 4 and 5. If constraints are incorporated in the model of the controller, the compensation speed for the applied step changes increases. Moreover since the control actions are limited to certain values and the process is highly interconnected the controller will try to compensate for this by making changes in the other control actions.

The EPSAC controller shows favourable performance, characterized by fast settling times, minimal undershoot and overshoot, and accurate reference tracking during consecutive reference changes. Being a multivariable control algorithm, it effectively manages input-output interdependencies, minimizing deviations from setpoints in other outputs when one output's reference changes.

Under constrained MPC conditions, the controller outputs stay within predefined limits. All changes presented in this work are both feasible and realistic within the regular operating circumstances of the considered process.

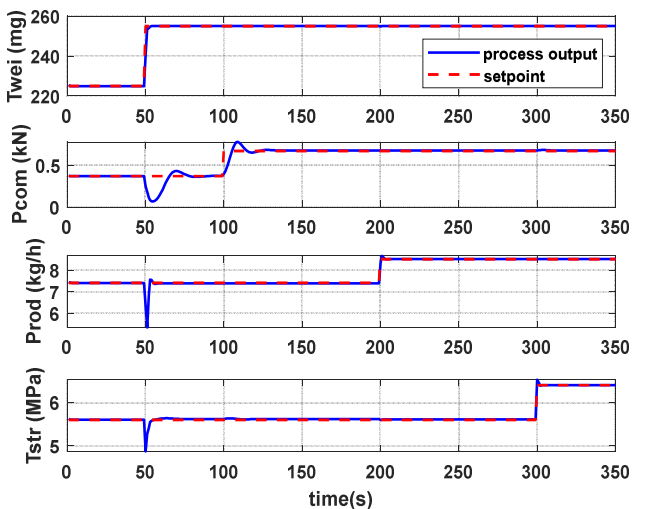


Fig. 4. Constraint reference tracking- process outputs

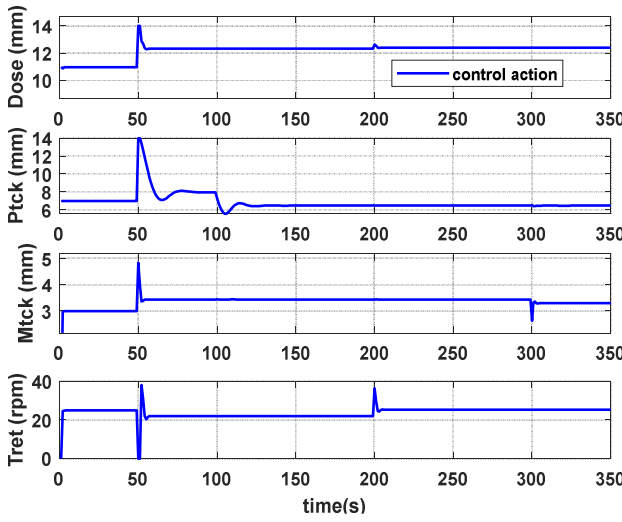


Fig. 5. Constraint reference tracking - controller outputs

B. Disturbance Rejection and Noise Influence

For an in-depth analysis of the closed-loop performances, transducers measurement noise is introduced into the process. For the noise simulation, a normally distributed zero mean and variance determined using historical plant data is included in the variability of the real sensor. Fig. 6 and 7 depict the controller performance results for the controlled variables as well as the control actions, respectively. It can be observed that despite the presence of noise, the developed EPSAC controller presents good performances, maintaining good dynamic and steady-state performance. If the design parameters are appropriately selected the oscillations that arise from the measurement noise can be attenuated while also keeping a balance between oscillations amplitude and the response time. To dampen these oscillations for all the controlled variables, controller aggressiveness on the corresponding loops has to be reduced which can be done by selecting suitable design parameters.

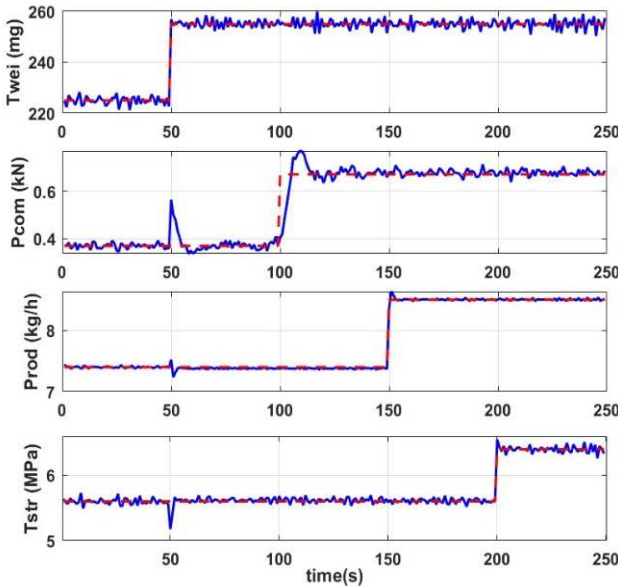


Fig. 6. Reference tracking – process outputs noisily

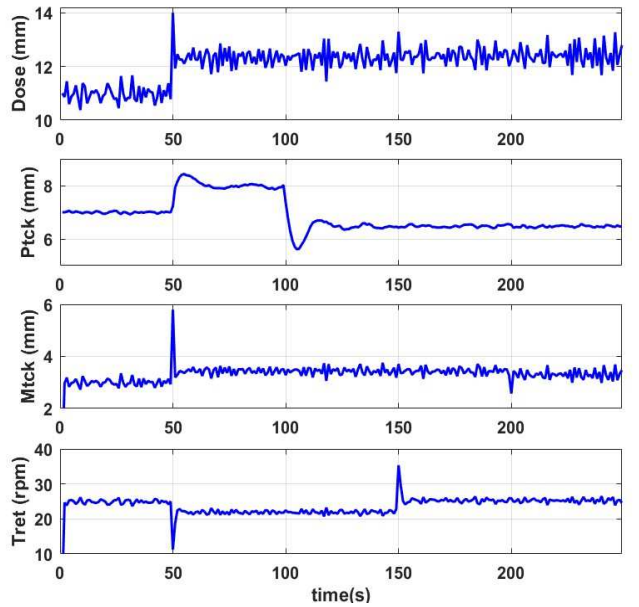


Fig. 7. Reference tracking – controller outputs considering the measurement noise

Monitoring the density of the powder bulk is critical in rotary tablet press operations, because it impacts the tablet characteristics. Moreover, disturbances may arise at any point and through any of the upstream unit operation such as: inside the feeder unit operation, throughout refill, while the feeder switches between gravimetric and volumetric mode. This can result in bulk density changes, either through compression (increased density) or aeration (decreased density) [15]. To implement the disturbance on the density of the bulk positive and negative step increases in the concentration of the silica are given: (i) at time $t=250$ seconds from the nominal value of 0.2% to 0.35% and (ii) at time $t=300$ seconds from 0.2% to 0.05%. To evaluate how the controller's performances are impacted by the direction of the disturbances, the chances in step are given in both directions.

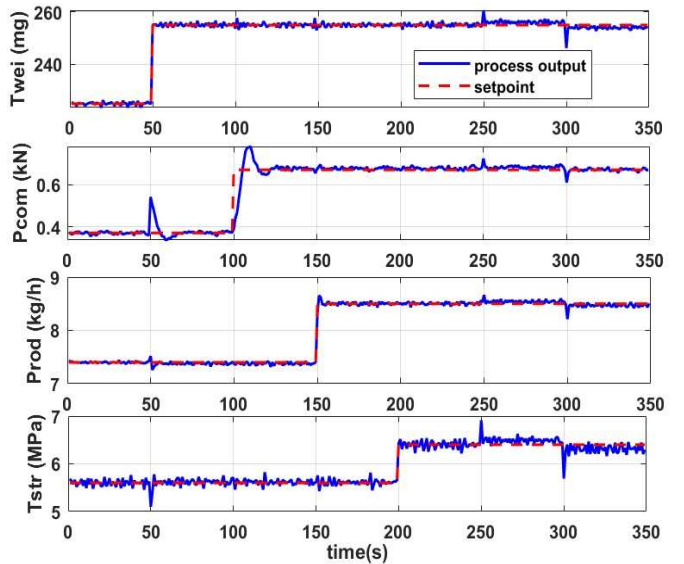


Fig. 8. Disturbance rejection – process outputs with sensor measurement noise

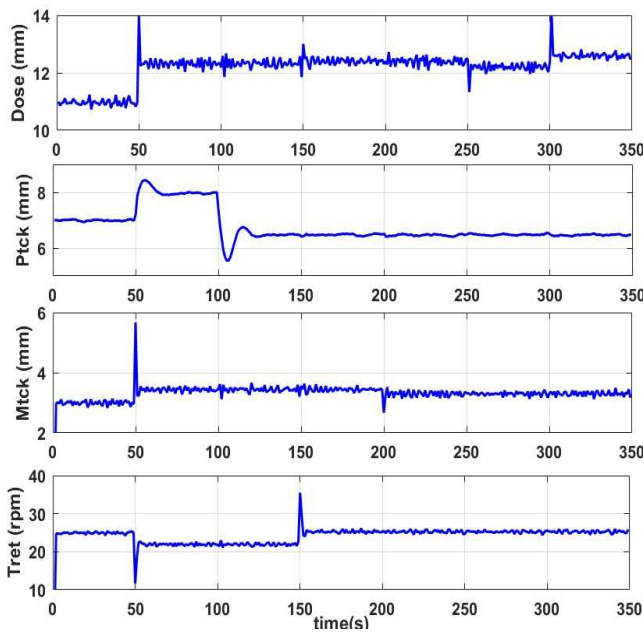


Fig. 9. Disturbance rejection - controller outputs with sensor measurement noise

The closed loop responses of the outputs of the process as well as the manipulated variables in the presence of these disturbances are presented in Fig. 8 and Fig. 9. The developed EPSAC control strategy shows good performances under disturbances, by bringing back the process to the imposed setpoint values.

To increase the performances of the controller, the model predictive controller can be given different tuning parameters. The aggressiveness and fast response of the developed controller response can be changed by choosing different prediction horizons and different penalties for the control actions.

IV. CONCLUSIONS

In alignment with the goals of Industry 4.0 and the transition to smart manufacturing, the pharmaceutical industry must adopt a Quality-by-Control approach. This research aims to develop, implement, and evaluate advanced model-based predictive control strategies for continuous pharmaceutical manufacturing in rotary tablet press processes, employing the Quality-by-Control paradigm.

The EPSAC model predictive controller developed in this study is implemented in a simulation environment using a high-fidelity model, that has been validated and calibrated

with pilot plant data. The controller's performance is assessed under both constrained and unconstrained conditions, focusing on (i) setpoint changes (e.g., variations in dosing position, pre-compression thickness, main compression thickness, and turret speed), (ii) sensor noise rejection, and (iii) bulk density disturbance rejection.

The developed EPSAC control strategies exhibit strong performance, with rapid settling times, minimal overshoot or undershoot, and no offset errors. These results hold true even under the influence of sensor noise and process disturbances, indicating enhanced process efficiency, greater flexibility, as well as a decreased environmental impact. The controller demonstrates robust performance even under uncertainties, noise, and disturbances, contributing to improved process reliability.

REFERENCES

- [1] Q. Su, S. Ganesh, D.B. Le Vo, A. Nukala, Y. Bommireddy, M. Gonzalez, G.V. Reklaitis, Z.K. Nagy, ESCAPE 46 (2019) 1327–1332.
- [2] Y. Chen, P. Bhalode, Y. Ou, M. Ierapetritou, in: Y. Yamashita, M. Kano (Eds.), Computer Aided Chemical Engineering, Elsevier, 2022, pp. 21–24.
- [3] Y.-S. Huang, M.Z. Sheriff, S. Bachawala, M. Gonzalez, Z.K. Nagy, G.V. Reklaitis, in: Y. Yamashita, M. Kano (Eds.), Computer Aided Chemical Engineering, Elsevier, 2022, pp. 2149–2154.
- [4] I. Naşcu, N.A. Diangelakis, S.G. Muñoz, E.N. Pistikopoulos, Computers & Chemical Engineering 173 (2023) 108212.
- [5] F. Destro, M. Barolo, International Journal of Pharmaceutics 620 (2022) 121715.
- [6] I. Naşcu, N.A. Diangelakis, E.N. Pistikopoulos, in: L. Montastruc, S. Negny (Eds.), Computer Aided Chemical Engineering, Elsevier, 2022, pp. 1159–1164.
- [7] Q. Su, S. Ganesh, M. Moreno, Y. Bommireddy, M. Gonzalez, G.V. Reklaitis, Z.K. Nagy, Computers & Chemical Engineering 125 (2019) 216–231.
- [8] I. Nascu, N. Diangelakis, Y.-S. Huang, Z. Nagy, I. Birs, I. Nascu, in: 2023, pp. 3540–3545.
- [9] N. Diangelakis, I. Pappas, E. Pistikopoulos, in: 2023, pp. 1711–1716.
- [10] E.N. Pistikopoulos, A. Barbosa-Povoa, J.H. Lee, R. Misener, A. Mitsos, G.V. Reklaitis, V. Venkatasubramanian, F. You, R. Gani, Computers & Chemical Engineering 147 (2021) 107252.
- [11] M. Ierapetritou, G. Reklaitis, F. Muzzio, AIChE Journal 62 (2016) n/a/n/a.
- [12] R.Z.C. de Meira, A.B. Maciel, F.S. Murakami, P.R. de Oliveira, L.S. Bernardi, Int J Anal Chem 2017 (2017) 2951529.
- [13] K. Kawakita, K.-H. Lüdde, Powder Technology 4 (1971) 61–68.
- [14] R. De Keyser, Invited Chapter in UNESCO Encyclopaedia of Life Support Systems (EoLSS) Article contribution 6.43.16.1 (2003).
- [15] C.A. Blackshields, A.M. Crean, Pharm Dev Technol 23 (2018) 554–560.